JOURNAL OF VIROLOGY, Apr. 2003, p. 4383–4388 Vol. 77, No. 7
0022-538X/03/$08.00+0 DOI: 10.1128/JVI.77.7.4383–4388.2003

NOTES

Apoptotic Cells, Including Macrophages, Are Prominent in Theiler's Virus-Induced Inflammatory, Demyelinating Lesions

Brian P. Schlitt,[1] Matthew Felrice,[1] Mary Lou Jelachich,[1] and Howard L. Lipton[1,2,3]*

Departments of Neurology,[1] Microbiology-Immunology,[2] and Biochemistry, Molecular Biology and Cell Biology,[3] Northwestern University, Evanston and Chicago, and Evanston Hospital, Evanston, Illinois 60201

Received 11 October 2002/Accepted 2 January 2003

Theiler's murine encephalomyelitis virus (TMEV) persists in the mouse central nervous system principally in macrophages, and infected macrophages in culture undergo apoptosis. We have detected abundant apoptotic cells in perivascular cuffs and inflammatory, demyelinating lesions of SJL mice chronically infected with TMEV. T cells comprised 74% of apoptotic cells, while 8% were macrophages, 0.6% were astrocytes, and ~17% remained unidentified. In situ hybridization revealed viral RNA in ~1% of apoptotic cells.

Theiler's murine encephalomyelitis virus (TMEV), a member of the *Cardiovirus* genus in the family *Picornaviridae*, produces a central nervous system (CNS) infection in mice leading to a chronic, inflammatory demyelinating pathology. TMEV preferentially replicates in CNS macrophages-microglia (hereafter, macrophages) during persistence and to a lesser extent in oligodendrocytes and astrocytes (11, 21, 26). A central role of macrophages in TMEV persistence was demonstrated by depletion of peripheral macrophages with mannosylated liposomes (26). One model of persistence involves macrophage-to-macrophage spread limited by a block(s) in virus replication as well as host antiviral immune responses but with dissemination to other cells, e.g., astrocytes and oligodendrocytes, where infection is cytolytic.

TMEV infection of macrophages in culture is dependent on the state of macrophage differentiation and activation (14, 29). Myelomonocytic precursors and activated macrophages are both resistant to infection, possibly due to the absence of coreceptors and increased innate immunity (14–16, 29; unpublished data). This limited window of susceptibility might account in part for the infection of only a small percentage of macrophages in the mouse spinal cord (11). Once infected, macrophages (both in mice and in cell culture) restrict TMEV replication at the level of viral assembly (11, 14, 18, 23).

TMEV-infected macrophages in culture undergo apoptosis (14, 23, 24, 29), either through an intrinsic pathway in nonactivated macrophages that requires virus replication and results in caspase activation or through an extrinsic pathway in gamma interferon-activated macrophages that involves signaling through receptors for tumor necrosis factor alpha and tumor necrosis factor alpha-related apoptosis-inducing ligand (16). However, the only report of apoptosis in TMEV infection of mice indicated that terminal deoxynucleotidyltransferase (TdT)-mediated UTP nick end labeling (TUNEL)-positive cells were seldom observed during viral persistence in the CNS (34), which suggests that apoptosis may be of little importance. Here, we report the detection of numerous apoptotic cells, primarily in the white matter in inflammatory demyelinating lesions in spinal cord sections of SJL mice chronically infected with BeAn virus.

Quantitation of apoptotic cells in spinal cords of mice with demyelinating disease. Cells in the spinal cords of 12 SJL mice inoculated intracerebrally with 10^6 PFU of BeAn virus and undergoing demyelination were assessed for apoptosis by TdT labeling according to the manufacturer's instructions (TdT-FrageEL kit; Oncogene, San Diego, Calif.). TdT-positive cells in cord sections were counted in four to six sections for each spinal cord segment by light microscopy.

Examination of spinal cord sections at three time points, representing increasingly severe disease, revealed 11.37 ± 1.80 (mean ± standard error [SE]) TUNEL-positive cells per section on day 31, 26.60 ± 3.40 cells on days 63 to 69, and 17.71 ± 2.67 cells on days 90 to 99 (Fig. 1A). The decreased mean number of apoptotic cells on days 90 to 99 did not differ significantly from that on days 63 to 69 ($P = 0.13$) and did not correlate with decreased pathological changes in these mice. Figure 2 shows the morphology and distribution of TUNEL-positive cells in a representative infected spinal cord section, as well as a control section. TUNEL-positive cells exhibited characteristic nuclear condensation indicative of apoptosis (Fig. 2E, arrows), and these cells tended to cluster at the periphery of demyelinating lesions (Fig. 2C). Figure 2B shows demyelination in a replicate section, where blue staining was reduced

* Corresponding author. Mailing address: Department of Neurology, Evanston Hospital, 2650 Ridge Ave., Evanston, IL 60201. Phone: (847) 570-2168. Fax: (847) 570-1568. E-mail: hllipton@merle.acns.nwu.edu.

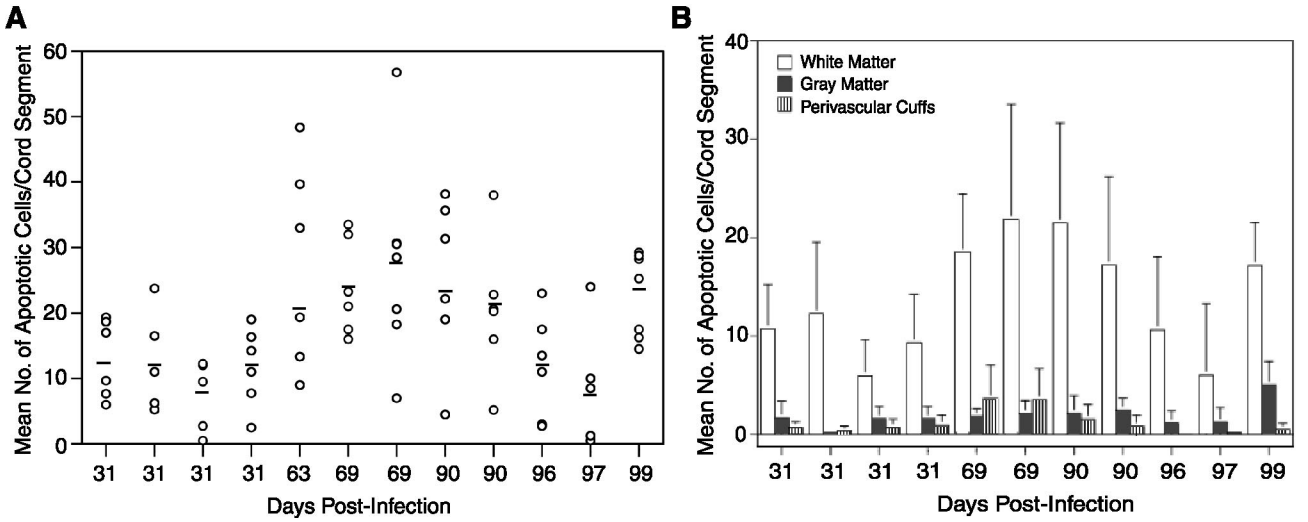

FIG. 1. (A) Number of apoptotic cells determined by TUNEL assay in spinal cord sections of BeAn virus-infected SJL mice during active demyelinating disease between days 31 and 99. Apoptotic cells in the leptomeninges were excluded from analysis. Shown are mean numbers (○) of TUNEL-positive cells in each spinal cord segment (four to six sections per segment) from mice sacrificed on the indicated days. Bars indicate the mean number of apoptotic cells for each mouse. (B) Number of apoptotic cells (means ± SEs) in different spinal cord locations determined by TUNEL assay in sections of BeAn virus-infected SJL mice during active demyelinating disease between days 31 and 99 (same mice as in panel A).

in affected areas; note the clustering of most TUNEL-positive cells in the anterior aspects of the lateral and ventral columns, areas typically affected earliest by inflammatory demyelination. Although no TUNEL-positive cells were observed in sections from uninfected control mice (Fig. 2A), spinal cord sections from infected mice were dual stained for TUNEL and anti-active caspase-3 to exclude the possibility of false-positive TUNEL reactivity (17, 30). TUNEL-positive and caspase-3-staining cells were observed in the same section, but the two stains rarely colocalized in a cell (data not shown). Although unexpected, the lack of colocalization may be explained by early caspase-3 degradation (12) as seen in BeAn virus-infected murine M1-D macrophages (unpublished data) and respiratory syncytial virus infection of epithelial cells (4). Activated caspase-3-stained cells (unlabeled polyclonal antibody CM1 to the C-terminal peptide of hCPP32; Idun Pharmaceutical, San Diego, Calif.) (31) were almost as frequent as TUNEL-positive cells in the same sections and had the same distribution (Fig. 3). This observation together with morphological features of apoptosis frequently displayed in the nuclei of TUNEL-stained cells indicated that programmed cell death was in fact induced in the persistently infected mice.

Distribution of apoptotic cells in spinal cords of mice with demyelinating disease. TUNEL-positive cells in the spinal cord white matter, perivascular cuffs, and gray matter were enumerated by using the same spinal cord segments as described above, except for the day 63 mouse sections, which were lost for this analysis (Fig. 1B). Because the leptomeninges were stripped from some sections, apoptotic cells detected in the leptomeninges were excluded from analysis (Fig. 2D). Significantly more apoptotic cells were found in the white matter than in perivascular cuffs ($P < 0.02$) and gray matter ($P < 0.01$) for all but the day 97 mouse ($P = 0.09$). Infection with cell culture-adapted BeAn virus results in limited neuronal death and inflammation in the gray matter that largely resolves by day 31 (20), probably accounting for the paucity of apoptotic cells in the gray matter. This distribution suggests that apoptosis is an integral part of the inflammatory demyelinating process.

Apoptotic cell phenotype. To determine the phenotype of TUNEL-positive cells, frozen spinal cord sections from four additional infected mice with signs of demyelinating disease (days 71, 84, 110, and 137) were stained with antibodies to T cells (fluorescein isothiocyanate-conjugated monoclonal antibodies to CD3 and CD8 [Serotec, Raleigh, N.C.] and CD4 [Caltag, Burlingame, Calif., and E-Biosciences, San Diego, Calif.]), macrophages (rat monoclonal antibody MOMA-2; George Kraal, Free University, Amsterdam, The Netherlands), and astrocytes (fluorescein isothiocyanate-glial fibrillary acidic protein [GFAP]; Molecular Probes, Eugene, Oreg.) and examined by light and digital confocal microscopy. Since macrophage epitopes were lost during fixation, paraffin-embedded sections were not used. Most TUNEL-positive cells were $CD3^+$, some were MOMA-2^+, and a few were $GFAP^+$ (Fig. 4A to C, respectively). Compared to the other nuclei, TUNEL-positive nuclei were usually condensed (Fig. 4). Quantitation of double-positive cells identified 73.98% ± 5.17% as T cells, 8.31% ± 2.91% as macrophages, and 0.56% ± 0.55% as astrocytes (Fig. 5); the remaining 17% of TUNEL-positive cells may include B cells and oligodendrocytes, but use of several commercially available antibodies to CD19 (BD PharMingen and E-Biosciences) and cyclic nucleotide phosphohydrolase (Sternberger Monoclonal Antibodies Inc., Lutherville, Md.) did not provide reliable results on frozen sections stained for TUNEL.

Low frequency of viral genomes in apoptotic cells. Analysis of paraffin-embedded spinal cord sections cut at 6 μm and mounted onto slides for BeAn virus RNA by in situ hybridiza-

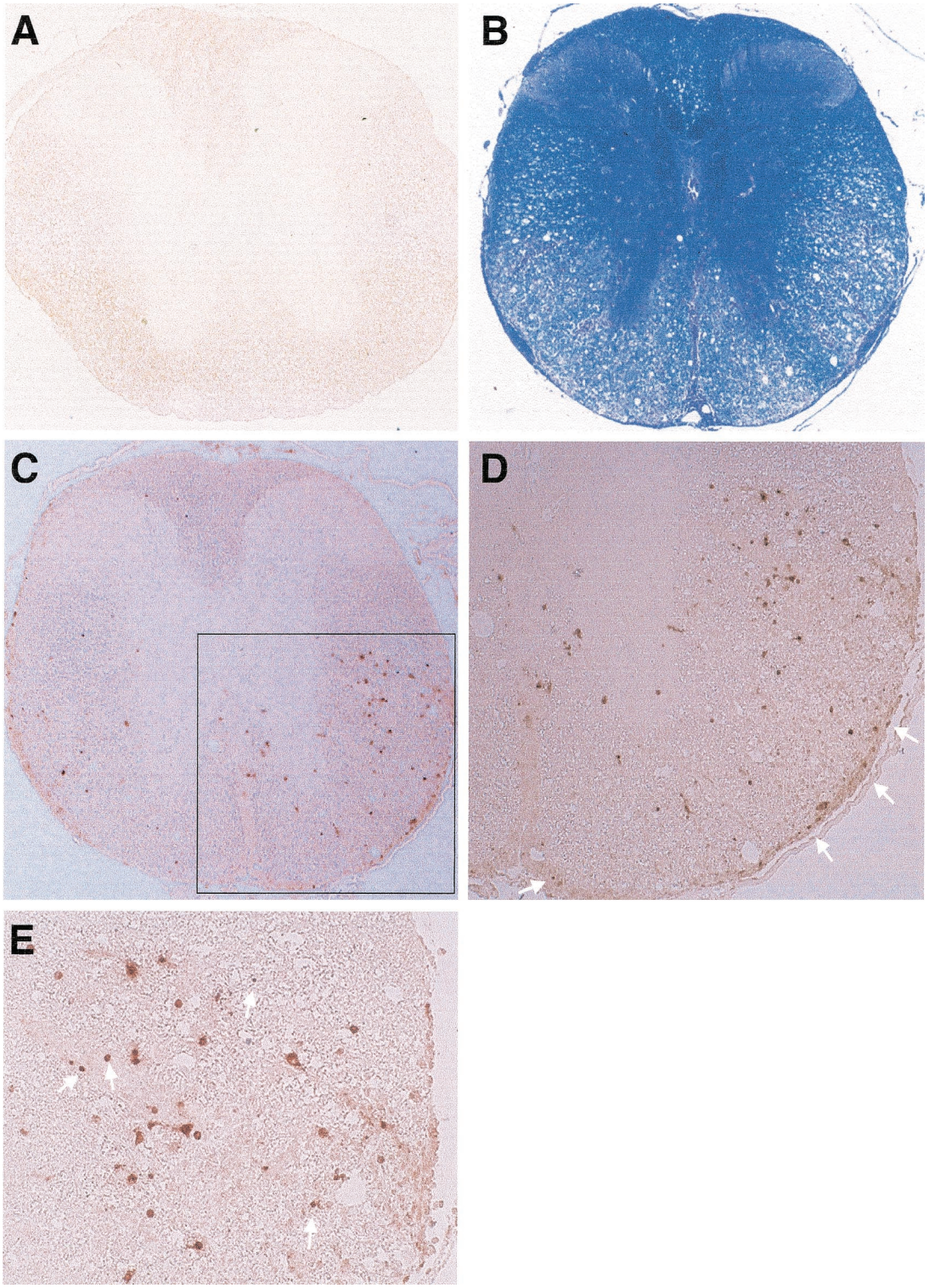

FIG. 2. Coronal spinal cord sections from a control mouse (A) and a BeAn virus-infected mouse sacrificed on day 69 (B to E). (B) Luxol fast blue staining reveals loss of myelin in the lateral and anterior columns; intense inflammatory infiltrates are visible in the leptomeninges in the ventral root entry zone and anterior commissure even at low-power magnification (×50). (C) Replicate section of panel B stained for TUNEL (no counterstaining), showing TUNEL-positive cells distributed in the white matter, especially anteriolaterally (magnification, ×50). (D) Magnification of the area boxed in panel C, showing distribution of TUNEL-positive cells around the periphery of a demyelinated area (compare with panel B). Arrows indicate TUNEL-positive cells in the pia layers of the leptomeninges (magnification, ×200). (E) Higher magnification (×400) of panel D, showing some TUNEL-positive cells exhibiting characteristic nuclear condensation indicative of apoptosis (arrows).

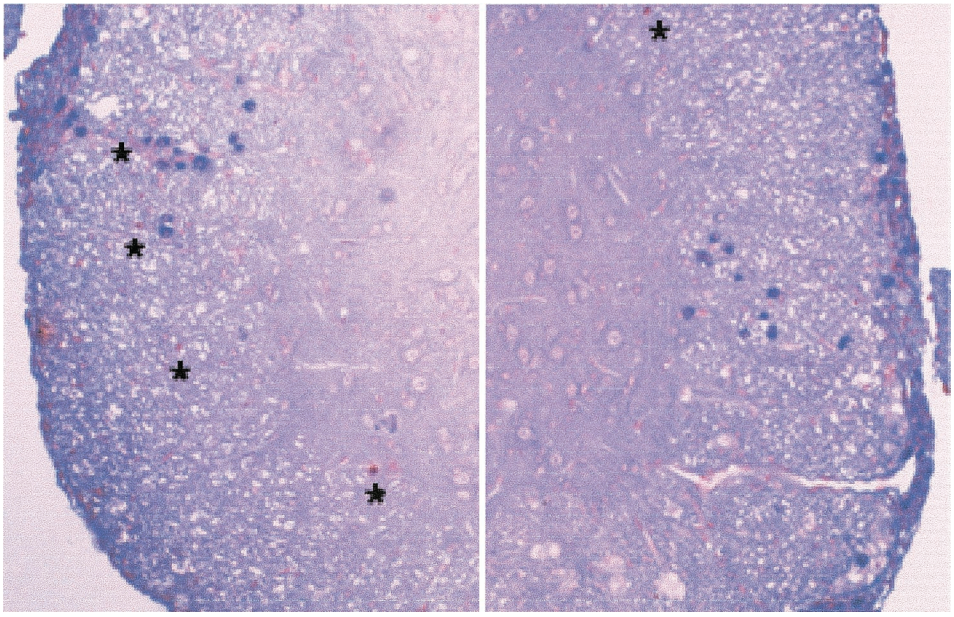

FIG. 3. Two activated caspase-3 (blue)- and TUNEL (brown)-stained cord sections from a BeAn virus-infected SJL mouse. Right panel, approximately 20 caspase-3-positive cells; left panel, about 25 caspase-3-positive cells in the white matter and leptomeninges; asterisks in both panels indicate several more prominently TUNEL-stained cells in the white matter (magnification, ×400). No caspase-3 staining was detected in sections from control mice (data not shown).

tion (32) and for apoptosis by TUNEL staining revealed viral RNA in ~1 in 100 TUNEL-positive cells in sections from five mice (three or four sections per cord segment for mice sacrificed on days 31, 63, 69, 90, and 99 [Fig. 1]). Figure 4D shows five TUNEL-positive cells (arrows), only one of which colocalized with viral RNA. This apoptotic cell is one of several heavily labeled cells clustered together; there are two other TUNEL-negative, infected cells with fewer grains in this cluster (asterisks). Previous in situ hybridization analysis identified two populations of infected cells, low (100 to 500)- and high (>1,000)-copy-number cells, in spinal cords of mice persistently infected with DA virus (8). The infected, apoptotic cell in Fig. 4D contained a high number of viral genomes. The phenotype of this cell was not determined because of its infrequency. Since half of peritoneal macrophages in vitro that undergo programmed cell death are infected (unpublished data; also supported by findings in reference 22) and assuming that most virus RNA-positive, apoptotic cells in this study were macrophages (T cells are not infected), one in four apoptotic macrophages would be expected to be infected.

Thus, the majority of apoptotic cells are uninfected and $CD3^+$, suggesting that apoptosis, at least in $CD3^+$ cells, is due to a mechanism other than that triggered by viral replication, probably activation-induced cell death because of the association with inflammation (3). Approximately one-third of TUNEL-positive cells were $CD8^+$ (data not shown), suggesting that the majority of apoptotic $CD3^+$ cells were $CD4^+$. However, we were unable to verify this with dual TUNEL and $CD4^+$ staining, using two different directly labeled antibodies. Nonetheless, our results are consistent with the literature demonstrating greater $CD4^+/CD8^+$ cell ratios in immunohistochemically stained sections (19) and in CNS mononuclear cells isolated from infected spinal cords, where $CD4^+$ cells also represent the majority of activated T cells (27).

Our results contrast with those of Tsunoda et al. (34) and E. L. Oleszak (personal communication), who found that apoptotic cells were rare in the spinal cords of mice persistently infected with DA virus. Possible explanations for this discrepancy are infection with different low-neurovirulence TMEV strains and a 10-fold-lower DA virus inoculum. However, two other reports with limited data suggest that TUNEL-positive cells may be more frequent (13, 28). In a study focused on $CD4^+$ T-cell-induced apoptosis of astrocytes in vitro, Palma et al. (25) reported a high level of TUNEL staining in hypertrophic fibrillary astrocytes and minimal staining of $CD4^+$ T cells in demyelinating lesions of BeAn virus-infected SJL mice at 120 days postinfection (p.i.), although quantitative data were not reported. During the time course of the present study, hypertrophic astrocytes were not observed, and only fibrillary processes and no enlarged astrocytic cell bodies were seen. In our infected SJL mice, hypertrophic astrocytes develop only after the mononuclear inflammatory process begins to resolve, usually ≥150 days p.i.

Tsunoda et al. (34) also reported that a small percentage of apoptotic cells in mice chronically infected with DA virus were immunoreactive with carbonic anhydrase II; however, the specificity of carbonic anhydrase II staining for oligodendrocytes is more reliable in normal rodent spinal cord than in reactive pathological conditions (6, 7). Although not confirmed in our study, oligodendrocytes could have been among the 17% of undefined apoptotic cells. Apoptosis has occurred only in restricted picornavirus infections (1). In contrast, TMEV replication in murine oligodendrocytes, unlike that in macro-

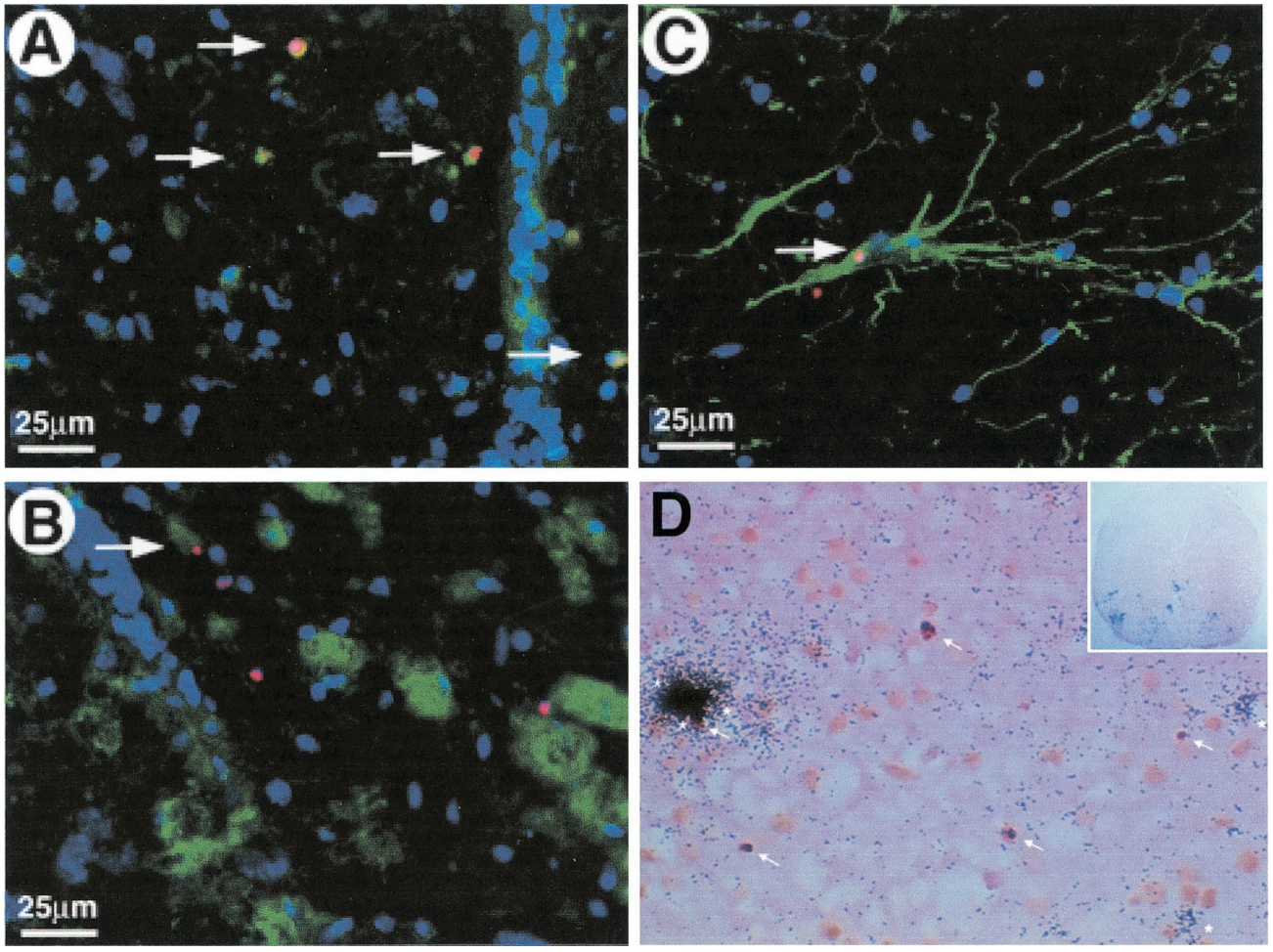

FIG. 4. Confocal images viewed with an Olympus IMT-2 microscope with digital deconvolution software of frozen spinal cord sections stained for nicked DNA (TUNEL, red); intact nuclei (4′,6′-diamidino-2-phenylindole, blue); and MOMA-2 (A), $CD3^+$ (B), and GFAP (C) fluorescein isothiocyanate-labeled antibodies (green) and light microscopy image of a representative paraffin section taken from a BeAn virus-infected spinal cord on day 63 analyzed by combined in situ hybridization for BeAn virus RNA and TUNEL staining (arrows) for apoptosis (D). Colocalized nuclear and nicked DNA in cells resulted in a yellow-orange color (one cell in panels A and C and four cells in panel B). For combined in situ hybridization for BeAn virus RNA and TUNEL staining (arrows) for apoptosis, antisense and sense ^{35}S-UTP-labeled BeAn virus probes (nucleotides 5967 to 6287) were synthesized with T7 and SP6 polymerase; probes with a specific activity of 6×10^7 cpm/μg in hybridization buffer were applied to tissue sections (D). In panel D, several cells (clustered together) on the extreme left have high viral RNA copy numbers (heavily grained area) and two separate cells on the lower right have low viral RNA copy numbers (asterisks). Only one infected, apoptotic cell, which is the bottommost cell in the cluster on the extreme left, is TUNEL positive (arrow; magnification, ×400). The insert shows the entire coronal spinal cord section from which the higher-power magnification field is taken; note grains over many cells in the anterior and lateral columns indicating the high level of viral persistence in this section (magnification, ×50).

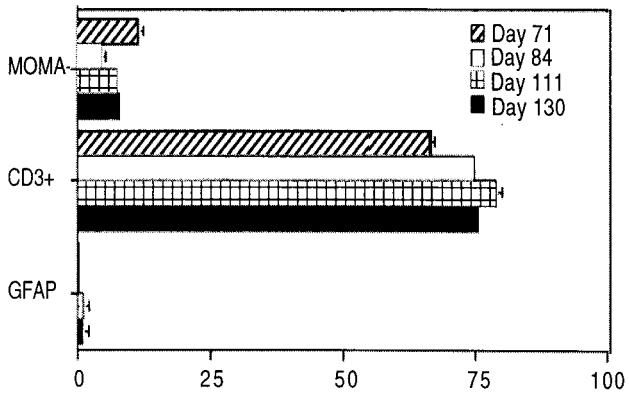

FIG. 5. Frequency of double-stained (antibodies to MOMA-2, CD3, or GFAP and to TUNEL) apoptotic cells in frozen spinal cord sections of four BeAn virus-infected SJL mice during persistent infection. The mean number (± SE) of double-positive cells identified as macrophages, T lymphocytes, and astrocytes per mouse is shown. In some instances, error bars were below graphic resolution.

phages, is highly productive and cytolytic in vitro (33, 35) and in vivo (5) and is less likely to result in apoptosis.

Apoptosis of infected macrophages may itself cause a block in virion assembly. The onset of caspase-3 activation (4 to 6 h p.i.) in infected, nonactivated M1-D cells coincides with the beginning of viral RNA replication (15, 16). Inhibition of ap-

optosis has been reported elsewhere to enhance viral yields in host cells for a number of viruses including human immunodeficiency virus (2, 9), simian immunodeficiency virus (2, 9), and adenovirus (10). Experiments are in progress to inhibit caspase activation in our macrophage cell lines to determine whether the block in BeAn virus replication is relieved. In animal hosts, restriction of virus replication by the host cell is a fundamental mechanism by which cytolytic RNA viruses persist. Thus, inhibition of apoptosis might alter the balance required for TMEV persistence in the CNS of mice. The availability of mice in which caspases have been inactivated promises to enable testing of this hypothesis in vivo.

We thank Lin Jing and Janelle Roby for help with in situ hybridization.

This work was supported by NIH grant NS 23349.

REFERENCES

1. **Agol, V. I., G. E. Belov, K. Bienz, D. Egger, M. S. Kolesnikova, L. I. Romanova, L. V. Sladkova, and E. A. Tolskaya.** 2000. Competing death programs in poliovirus-infected cells: commitment switch in the middle of the infectious cycle. J. Virol. **74:**5534–5541.
2. **Antoni, B. A., P. Sabbatini, A. B. Rabson, and E. White.** 1995. Inhibition of apoptosis in human immunodeficiency virus-infected cells enhances virus production and facilitates persistent infection. J. Virol. **69:**2384–2392.
3. **Bauer, J., M. Bradl, W. F. Hickey, F. Forss-Petter, H. Breitschopf, C. Linnington, H. Wekerle, and H. Lassmann.** 1998. T cell apoptosis in inflammatory brain lesions: destruction of T cells does not depend on antigen recognition. Am. J. Pathol. **153:**715–724.
4. **Bitko, V., and S. Barik.** 2001. An endoplasmic reticulum-specific stress-activated caspase (caspase-12) is implicated in the apoptosis of A549 epithelial cells by respiratory syncytial virus. J. Cell. Biochem. **80:**441–454.
5. **Blakemore, W. F., C. J. Welsh, P. Tonks, and A. A. Nash.** 1988. Observations on demyelinating lesions induced by Theiler's virus in CBA mice. Acta Neuropathol. **76:**581–589.
6. **Cammer, W., and F. A. Tansey.** 1988. Carbonic anhydrase immunostaining in astrocytes in the rat cerebral cortex. J. Neurochem. **50:**319–322.
7. **Cammer, W., and H. Zhang.** 1991. Comparison of immunocytochemical staining of astrocytes, oligodendrocytes, and myelinated fibers in the brains of carbonic anhydrase II-deficient mice and normal littermates. J. Neuroimmunol. **34:**81–86.
8. **Cash, E., M. Chamorro, and M. Brahic.** 1985. Theiler's virus RNA and protein synthesis in the central nervous system of demyelinating mice. Virology **144:**290–294.
9. **Chinnaiyan, A. M., C. Woffendin, V. Dixit, and G. Nabel.** 1997. The inhibition of pro-apoptotic ICE-like proteases enhances HIV replication. Nat. Med. **3:**333–337.
10. **Chiou, S.-K., and E. White.** 1998. Inhibition of ICE-like proteases inhibits apoptosis and increases virus production during adenovirus infection. Virology **244:**108–118.
11. **Clatch, R. J., S. D. Miller, R. Metzner, M. C. Dal Canto, and H. L. Lipton.** 1990. Monocytes/macrophages isolated from the mouse central nervous system contain infectious Theiler's murine encephalomyelitis virus (TMEV). Virology **176:**244–254.
12. **Collins, J. A., C. A. Schandl, K. K. Young, J. Vesely, and M. C. Willingham.** 1997. Major DNA fragmentation is a late event in apoptosis. J. Histochem. Cytochem. **45:**923–934.
13. **Drescher, K. M., P. D. Murray, X. Lin, J. A. Carlino, and M. Rodriguez.** 2000. TGF-β2 reduces demyelination, virus antigen expression and macrophage recruitment in a viral model of multiple sclerosis. J. Immunol. **164:**3207–3213.
14. **Jelachich, M. L., P. Bandyopadhyay, K. Blum, and H. L. Lipton.** 1995. Theiler's virus growth in murine macrophage cell lines depends on the state of differentiation. Virology **209:**437–444.
15. **Jelachich, M. L., C. Brumlage, and H. L. Lipton.** 1999. Differentiation of M1 myeloid precursor cells into macrophages results in binding and infection by Theiler's murine encephalomyelitis virus and apoptosis. J. Virol. **73:**3227–3235.
16. **Jelachich, M. L., and H. L. Lipton.** 2001. Theiler's murine encephalomyelitis virus induces apoptosis in gamma interferon-activated M1 differentiated myelomonocytic cells through a mechanism involving tumor necrosis factor alpha (TNF-α) and TNF-α-related apoptosis-inducing ligand. J. Virol. **75:**5930–5938.
17. **Labat-Moleur, F., C. Guillermet, P. Lorimier, C. Robert, S. Lantuejoul, E. Brambilla, and A. Negoescu.** 1998. TUNEL apoptotic cell detection in tissue sections: critical evaluation and improvement. J. Histochem. Cytochem. **46:**327–334.
18. **Levy, M., C. Aubert, and M. Brahic.** 1992. Theiler's virus replication in brain macrophages cultured in vitro. J. Virol. **66:**3188–3193.
19. **Lindsley, M. D., and M. Rodriguez.** 1989. Characterization of the inflammatory response in the central nervous system of mice susceptible or resistant to demyelination by Theiler's virus. J. Immunol. **142:**2677–2682.
20. **Lipton, H. L.** 1975. Theiler's virus infection in mice: an unusual biphasic disease process leading to demyelination. Infect. Immun. **11:**1147–1155.
21. **Lipton, H. L., G. Twaddle, and M. L. Jelachich.** 1995. The predominant virus antigen burden is present in macrophages in Theiler's murine encephalomyelitis virus-induced demyelinating disease. J. Virol. **69:**2525–2533.
22. **Martinat, C., I. Mena, and M. Brahic.** 2002. Theiler's virus infection of primary cultures of bone marrow-derived monocytes/macrophages. J. Virol. **76:**12823–12833.
23. **Obuchi, M., Y. Ohara, T. Takegami, T. Murayama, H. Takada, and H. Iizuka.** 1997. Theiler's murine encephalomyelitis virus subgroup strain-specific infection in a murine macrophage-like cell line. J. Virol. **71:**729–733.
24. **Ohara, Y., T. Himeda, K. Asakura, and M. Sawada.** 2002. Distinct death mechanisms by Theiler's murine encephalomyelitis virus (TMEV) infection in microglia and macrophage. Neurosci. Lett. **327:**41–44.
25. **Palma, J. P., R. L. Yauch, S. Lang, and B. S. Kim.** 1999. Potential role of $CD4^+$ T cell-mediated apoptosis of activated astrocytes in Theiler's virus-induced demyelination. J. Immunol. **162:**6543–6551.
26. **Pena Rossi, C., M. Delcroix, I. Huitinga, A. McAllister, N. van Rooijen, E. Claassen, and M. Brahic.** 1997. Role of macrophages during Theiler's virus infection. J. Virol. **71:**3336–3340.
27. **Pope, J. G., W. J. Karpus, C. VanderLugt, and S. D. Miller.** 1996. Flow cytometric and functional analyses of central nervous system-infiltrating cells in SJL/J mice with Theiler's virus-induced demyelinating disease. J. Immunol. **156:**4050–4058.
28. **Rose, J. W., K. E. Hill, Y. Wada, C. I. B. Kurtz, I. Tsunoda, R. S. Fujinami, and A. H. Cross.** 1998. Nitric oxide synthase inhibitor, aminoguanidine, reduces inflammation and demyelination produced by Theiler's virus infection. J. Neuroimmunol. **81:**82–89.
29. **Shaw-Jackson, C., and T. Michiels.** 1997. Infection of macrophages by Theiler's murine encephalomyelitis virus is highly dependent on their activation or differentiation state. J. Virol. **71:**8864–8867.
30. **Sloop, G. D., J. C. Roa, A. G. Delgado, J. T. Balart, M. O. Hines III, and J. M. Hill.** 1999. Histologic sectioning produces TUNEL reactivity. Arch. Pathol. Lab. Med. **123:**529–532.
31. **Srinivasan, A., K. A. Roth, R. O. Sayers, K. S. Shindler, A. M. Wong, L. C. Fritz, and K. J. Tomaselli.** 1998. In situ immunodetection of activated caspase-3 in apoptotic neurons in the developing nervous system. Cell Death Differ. **5:**1004–1016.
32. **Suhr, S. T., J. O. Rahal, and K. E. Mayo.** 1989. Mouse growth hormone-releasing hormone: precursor structure and expression in brain and placenta. Mol. Endocrinol. **3:**1693–1700.
33. **Trottier, M., P. Kallio, W. Wang, and H. L. Lipton.** 2001. High numbers of viral RNA copies in the central nervous system of mice during persistent infection with Theiler's virus. J. Virol. **75:**7420–7428.
34. **Tsunoda, I., C. I. B. Kurtz, and R. S. Fujinami.** 1997. Apoptosis in acute and chronic central nervous system disease induced by Theiler's murine encephalomyelitis virus. Virology **228:**388–393.
35. **Zheng, L., M. A. Calenoff, and M. C. Dal Canto.** 2001. Astrocytes, not microglia, are the main cells responsible for viral persistence in Theiler's murine encephalomyelitis virus infection leading to demyelination. J. Neurovirol. **118:**256–267.